Mechanisms underlying drug-mediated regulation of membrane protein function

Radda Rusinova, Changhao He and Olaf S. Andersen

Supplemental Tables and Figures

Table S1

Drug	logK_P	Source	#Structure	†Clinical concentrations (μM)	[Drug]$_{nom}$ = 10 μM	
					m_D	[Drug]$_m$ (μM)
amiodarone	4.4	(Fig. S9)	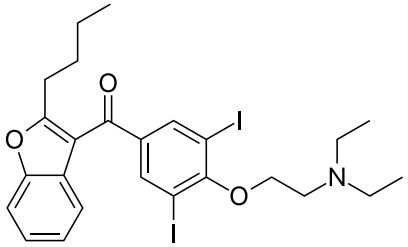	[a] 1	0.034	34,000
propranolol	2.8	(Fig. S9)	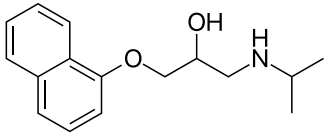	[b] 0.1-1	0.005	5,000
pindolol	*1.8	(41)	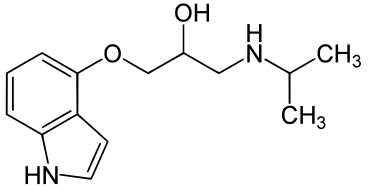	[c] 0.04	0.004	4,000

Drug	logK_P	Source	#Structure	†Clinical concentrations (μM)	[Drug]$_{nom}$ = 10 μM	
					m_D	[Drug]$_m$ (μM)
troglitazone	4.3	(Fig. S9)(9)	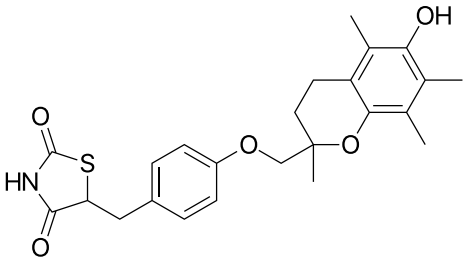	[d] 2–6.4	0.033	33,000
TX-100	4.1	(38)	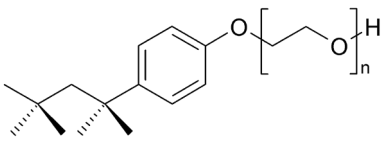		0.03	30,000
fluoxetine	3.6	(39)	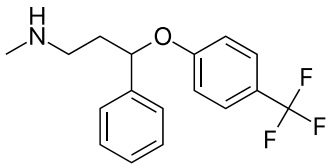	[e] 0.1-1	0.02	20,000
pioglitazone	*3.1	(75)	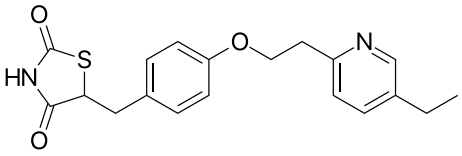	[f] 1.5–4.4	0.013	13,000

Drug	logK_P	Source	#Structure	†Clinical concentrations (µM)	[Drug]$_{nom}$ = 10 µM	
					m_D	[Drug]$_m$ (µM)
TBA			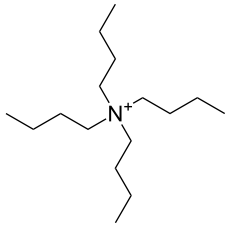			

Structures rendered using MarvinSketch (ChemAxon); *determined from water/octanol partitioning; †The free aqueous concentrations will be less than the nominal concentrations because drug redistribution between the aqueous solution and other compartments, like the bilayer, will decrease the aqueous concentration, e.g., (9). m_D – mole fraction, [Drug]$_m$ – concentration of drug in the lipid bilayer

[a](76) et al. (1983), (77) et al. (1984), and (78) (2003).[b](79) et al. (1979), (80) et al. (1982), and (78) (2003).

[c](81) et al. (1994) and (82) (2001). [d]FDA. [e](83), 1999; (84), 2007,[f](85) et al., 2003.

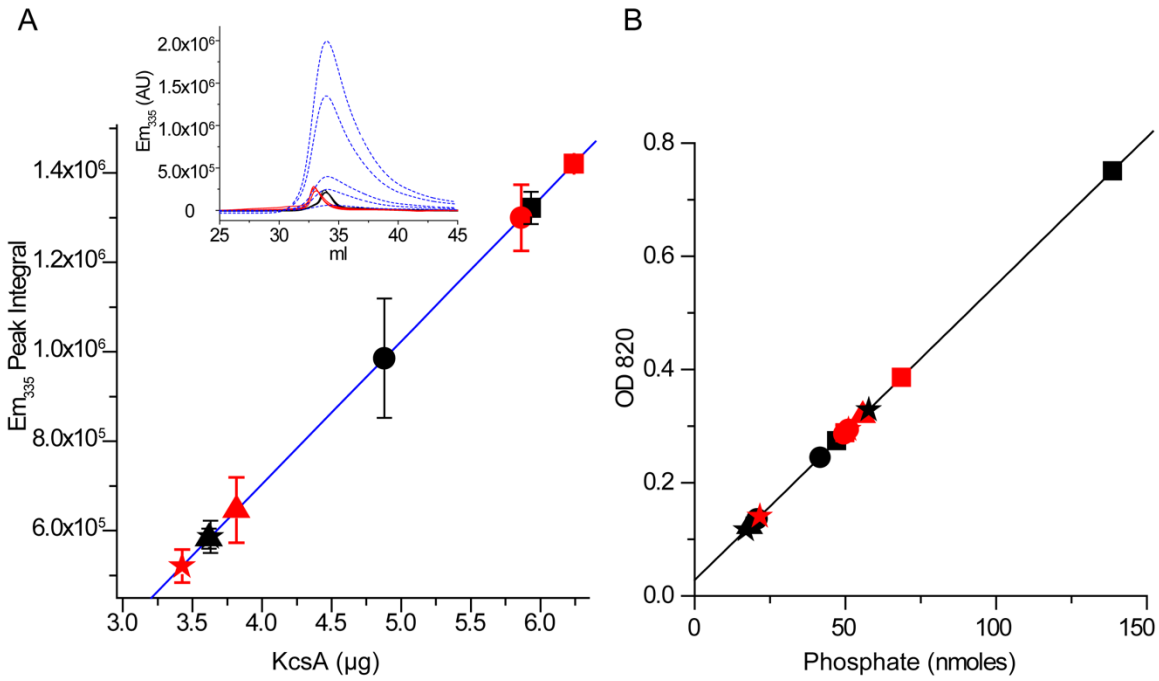

C

	Batch 1		Batch 2		Batch 3		Batch 4	
	$C_{22:1}$	$C_{18:1}$	$C_{22:1}$	$C_{18:1}$	$C_{22:1}$	$C_{18:1}$	$C_{22:1}$	$C_{18:1}$
Lipid (M)	$6.7 \cdot 10^{-3}$	$4.6 \cdot 10^{-3}$	$3.9 \cdot 10^{-3}$	$4.8 \cdot 10^{-3}$	$3.8 \cdot 10^{-3}$	$4.9 \cdot 10^{-3}$	$4.3 \cdot 10^{-3}$	$4.7 \cdot 10^{-3}$
LUV (M)	$5.7 \cdot 10^{-8}$	$2.9 \cdot 10^{-8}$	$3.2 \cdot 10^{-8}$	$3.0 \cdot 10^{-8}$	$3.2 \cdot 10^{-8}$	$3.0 \cdot 10^{-8}$	$3.6 \cdot 10^{-8}$	$2.9 \cdot 10^{-8}$
KcsA (ng)	178	187	146	176	109	115	109	103
KcsA/LUV	15	30	20	27	16	17	14	16

Supplemental Figure S1.

Supplemental Figure S1. Determining the amount of KcsA reconstituted into $C_{22:1}$ or $C_{18:1}$. (A) SEC determination of KcsA in each of the four batches of $C_{22:1}$ and $C_{18:1}$. To estimate the amount of KcsA in each batch, we calibrated the signal with varying amounts (1 – 100 μg) of purified KcsA in 5 mM DDM. The top inset shows the tryptophan emission signal for known amounts of purified KcsA (blue dashed lines) and for KcsA reconstituted into $C_{22:1}$ (black lines) and $C_{18:1}$ (red lines); both were done in triplicate. The symbols on the main graph denote integrated peak areas for the LUV-reconstituted KcsA. The blue line denotes the calibration curve determined using purified KcsA; the amounts of KcsA in $C_{22:1}$ (black symbols) and $C_{18:1}$ (red symbols) were estimated from the calibration curve. The square, circle, triangle and star symbols correspond to batches 1-4 as in panel (A). (B) Calibration curve for phosphate assay (black line) used to measure the amount of lipid in $C_{18:1}$ (red symbols) or $C_{22:1}$ (black symbols), the amount of lipid in each batch of reconstituted vesicles was determined from a linear fit to the calibration. Four batches were tested (each symbol represents different amount of lipid loaded from the same batch and each symbol shape represents a different batch). (C) The amounts of lipid and KcsA determined for each batch and the resulting number of KcsA per LUV. Molar concentration of LUVs was calculated by dividing the molar amount of lipid in each batch as measured using the phosphate assay by the number of molecules required to form an LUV with radii of 58 ± 1 nm, for $C_{22:1}$, or 66 ± 1 nm, for $C_{18:1}$ (Mean ± range/2, n = 2) as determined by Dynamic Light Scattering (Litesizer500, Anton Paar, Graz, Germany).

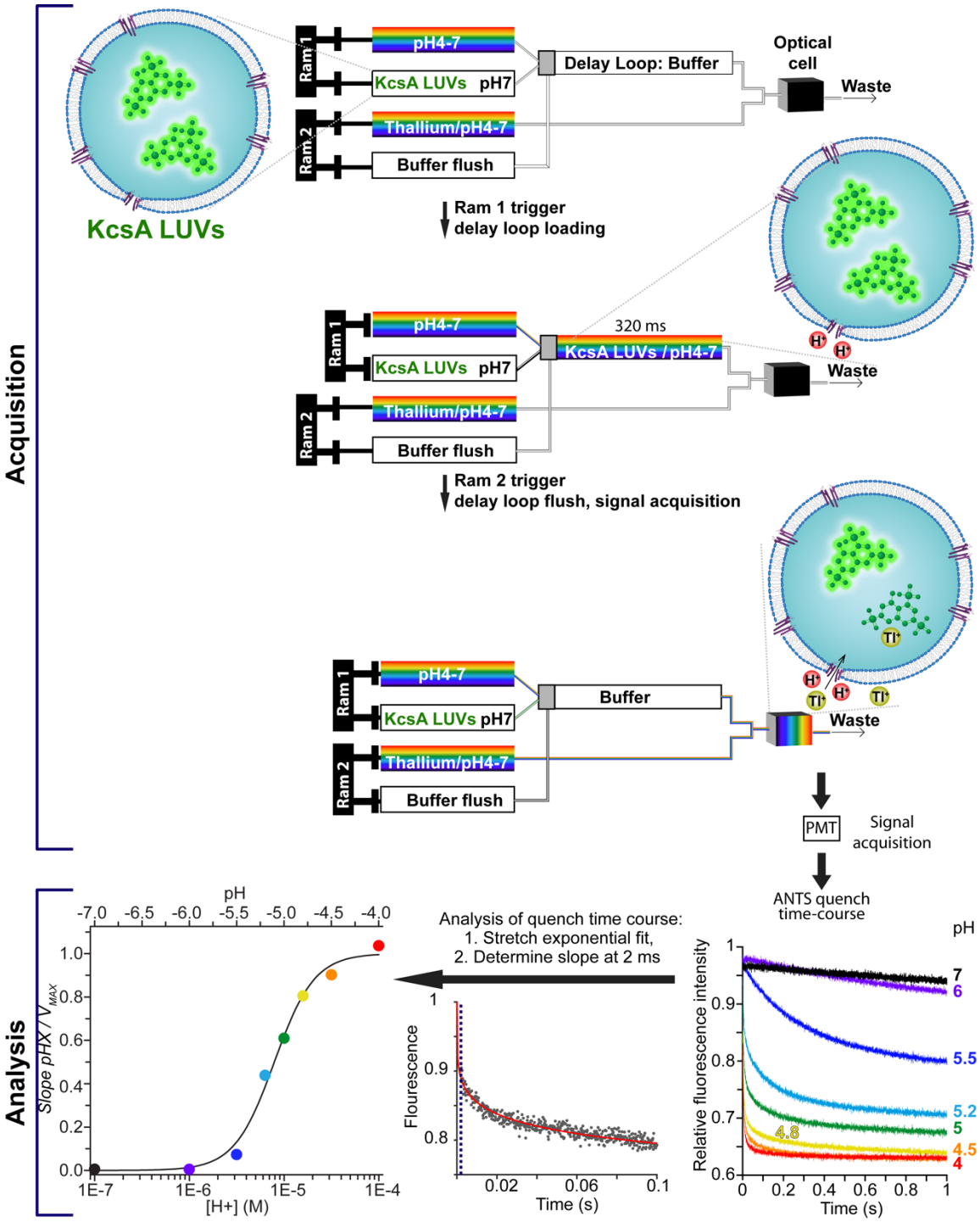

Supplemental Figure S2.

Supplemental Figure S2. Experimental design for determining the KcsA H^+ dose-response curves. Top **Data Acquisition**: LUV-reconstituted KcsA at pH 7 and a buffer solution with a pH that sets the pH KcsA is exposed to in the delay loop are loaded into two separate syringes that are activated by Ram 1. Triggering Ram 1 fills the delay loop and combines the KcsA LUVs and the buffer solution at a 1:1 ratio in the delay loop at the desired $[H^+]$ (red spheres) for 320 ms, when KcsA at the set pH is mixed with Tl^+ (yellow spheres) in the optical cell by the subsequent triggering of Ram 2. Tl^+ enters the LUVs via open KcsA which quenches the ANTS fluorescence. Bottom: **Data Analysis** (read from right to left): The time course of the ANTS quenching by Tl^+ is recorded; the traces show averaged traces from multiple repeats at each pH. The center graph represents a single repeat (dots) of the above experiment and analyzed by fitting to a stretched exponential function (red solid line) and determining the slope at 2 ms. Several repeats are recorded at each pH and the experiment is repeated at a different pH values to collect the desired series. The mixing repeats recorded at each pH are averaged (right graph) to show how the quench time courses differ as function of pH. The slopes from each repeat at one pH reflect KcsA activity at those conditions; the vales are averaged, plotted as a function of pH and fit by a Hill function $Activity = \frac{[H^+]^{n_H}}{10^{-n_H \cdot pH_{0.5}} + [H^+]^{n_H}}$.

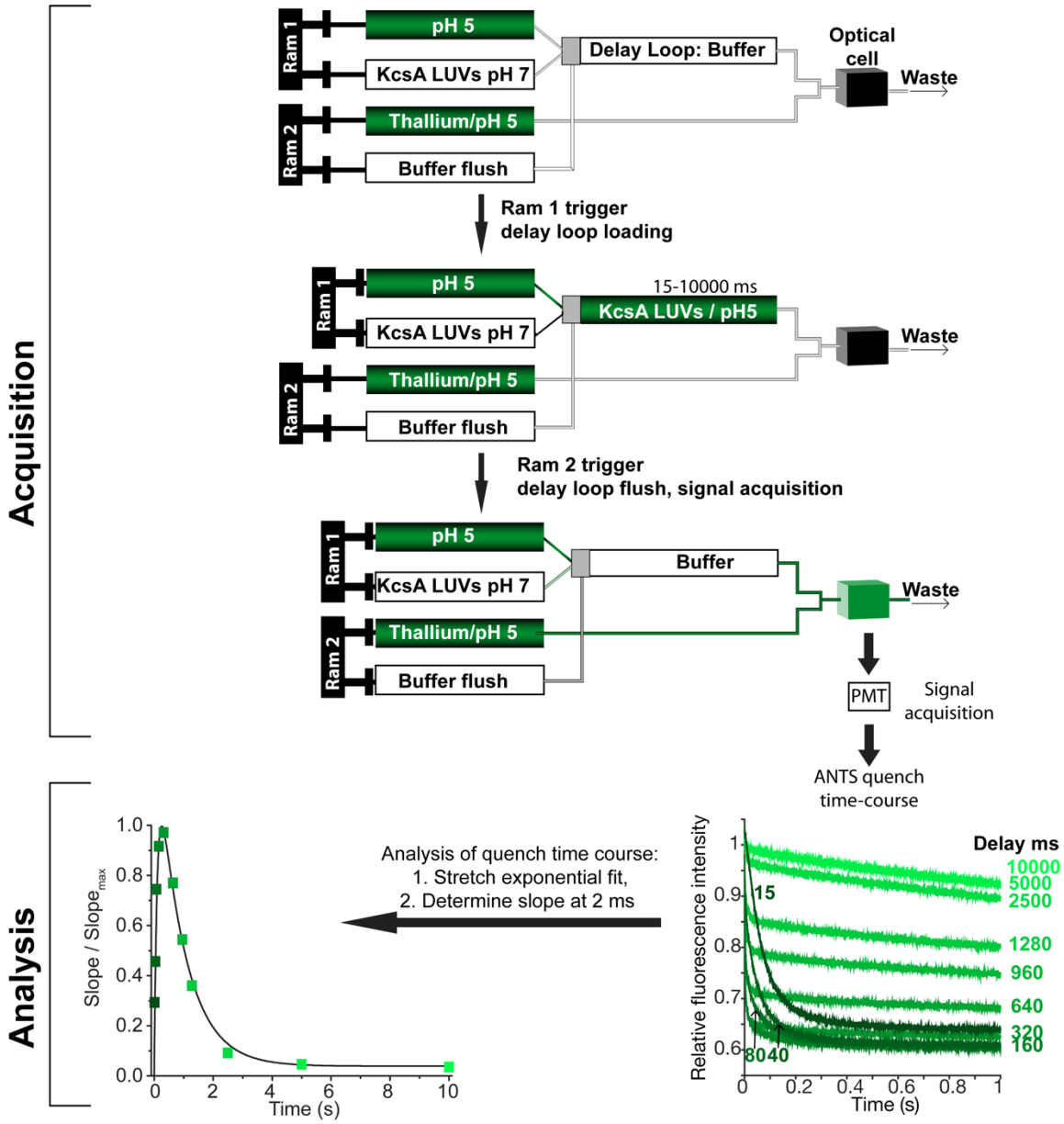

Supplemental Figure S3.

Supplemental Figure S3. Experimental design for determining KcsA activation and inactivation time-courses. **Data acquisition**: As in Fig. S2, LUV-reconstituted KcsA at pH 7 and a buffer solution with a pH (3.9) adjusted so that KcsA is exposed to 10 μM H^+ in the delay loop are loaded in separate syringes that are activated by Ram 1. KcsA is incubated in the delay loop at pH 5 for durations between 15 ms and 10 s, which allows for probing the activated KcsA population as function of time. To test for KcsA activity after the desired duration, activation of Ram2 mixes KcsA with Tl^+ (yellow spheres) in the optical cell while recording the ANTS quench time course. Several repeats for each duration are recorded. **Data analysis**: The resulting quench time courses from each repeat are fit with a stretched exponential function and the slope at 2 ms is determined. The graph at the bottom right shows averages of several repeats for different incubations at pH 5 in the delay loop showing first increase in quenching as KcsA activates and followed by reduction as it inactivates. The graph at the bottom left shows averages of the initial slopes of the quench time courses from the fits as function of duration in the delay loop.

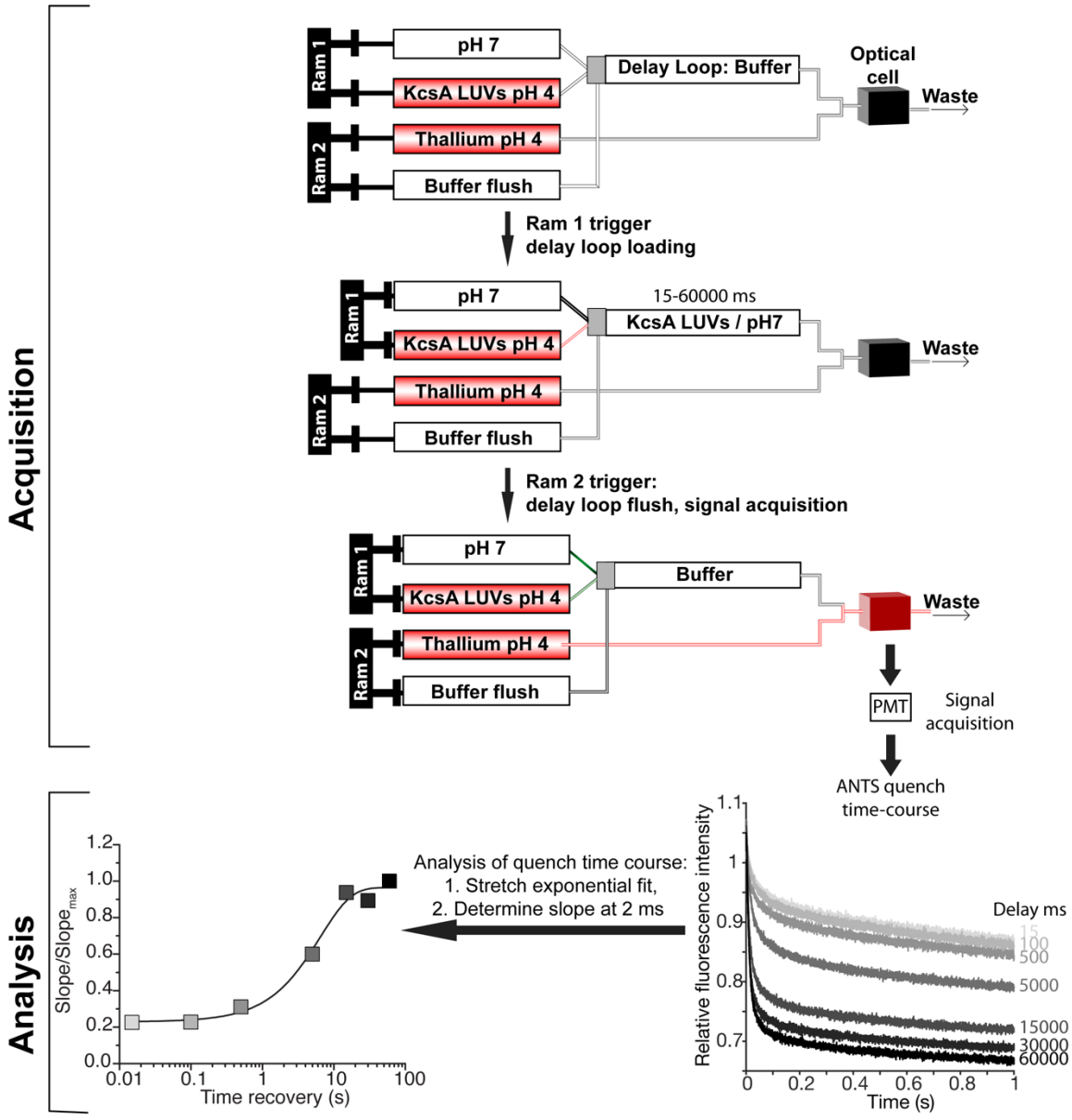

Supplemental Figure S4.

Supplemental Figure S4. Experimental design for determining the time-course of KcsA recovery from inactivation. **Data Acquisition**: As in Figs. S2 and S3, LUV-reconstituted KcsA at pH 4 (red spheres) and buffer solution are loaded in separate syringes. Ram 1 mixes the KcsA (pH 4.0) and buffer solution (pH 11.9), which results in pH 7 in the delay loop when mixed 1:1. KcsA is exposed to pH 7 for durations between 15 ms to 60 s, which allows for probing the recovery at each time point by activating Ram 2, which will mix the solution in the delay loop with a Tl^+ (yellow spheres) solution at pH 2.3, so that KcsA is exposed to pH 4 in the optical cell while recording the time course of ANTS quench. For each duration, several repeats are recorded, and quench time courses from each repeat are fit using stretched exponential function and the slope at 2 ms is determined. **Data Analysis** (read from right to left): The graph at the bottom right shows averages of several repeats for each duration at pH 5 in the delay loop, showing an increase in the fractional quench as KcsA recovers from inactivation as function of time at pH 7. The graph at the bottom left shows averages of the initial slopes of the quench curves (from the stretched exponential fits), as a function of duration in the delay loop (time at pH 7), which maps the time course of KcsA recovery from inactivation.

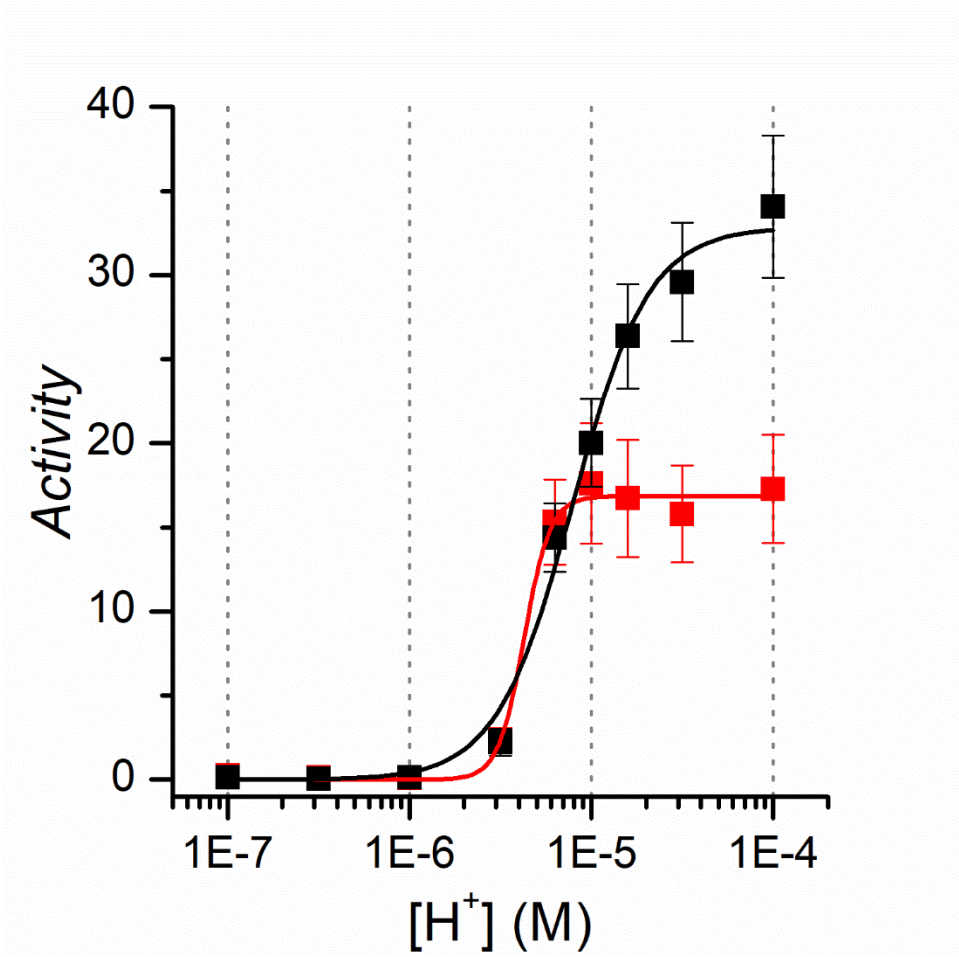

Supplemental Figure S5. H^+ dose-response curves for KcsA reconstituted in $C_{22:1}$ (black squares) and $C_{18:1}$ (red squares). Data points represent the average non-normalized slopes ± SEM, n = 5 – 7; the solid curves denote the Hill fits for each data set (black curve for $C_{22:1}$, red curve for $C_{18:1}$) yielding $pH_{0.5}$ and n_H estimates of 5.39 ± 0.02, 6.1 ± 0.8 for $C_{18:1}$ and 5.10± 0.03, 2.1 ± 0.3 for $C_{22:1}$.

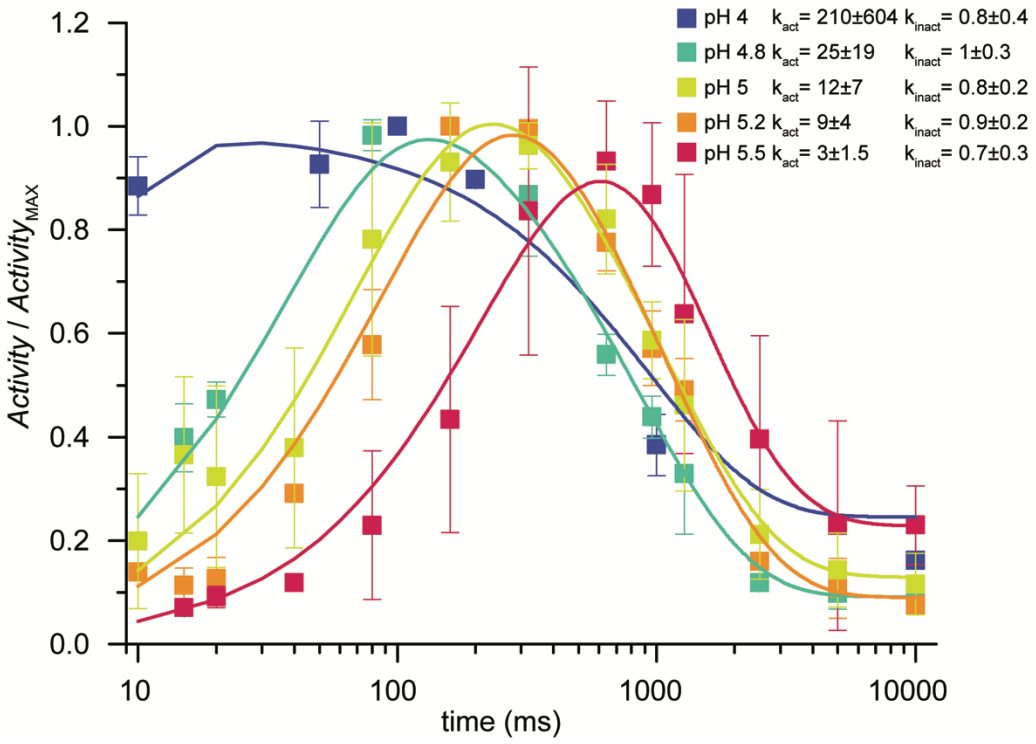

Supplemental Figure S6: Time course of activation and inactivation of KcsA reconstituted in $C_{18:1}$ at pHs ranging between 4 and 5.5. Slopes obtained at each time point for each pH was normalized to the maximum slope for that pH. Data points (squares) denote Mean ± SEM for n = 3 – 12, or Mean ± range for n = 2. Data were fit by a 3-state model using QuB. The fits are shown as solid lines.

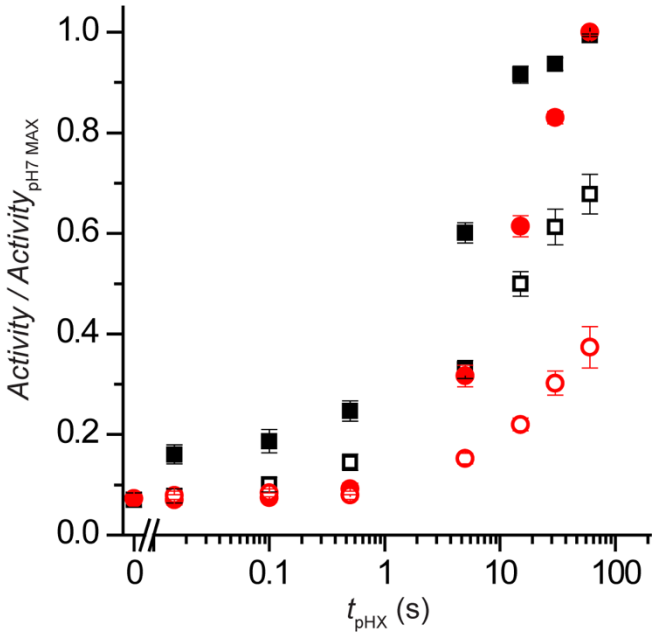

Supplemental Figure S7. Recovery from inactivation at pH 7 (closed symbols) and 5.2 (open symbols) for KcsA reconstituted in $C_{22:1}$ (black symbols) and $C_{18:1}$ (red symbols). The rate of recovery from inactivation at pH 5.2 was determined using the protocol in Fig. S3 (except that the pH in the delay loop was pH 5.2 rather than 7). The activity at each time point is normalized to the activity after recovery at pH 7 for 60 s ($Activity/Activity_{pH7,max}$) and plotted as function of time in the delay loop. The pH 7 results are from Fig. 1D.

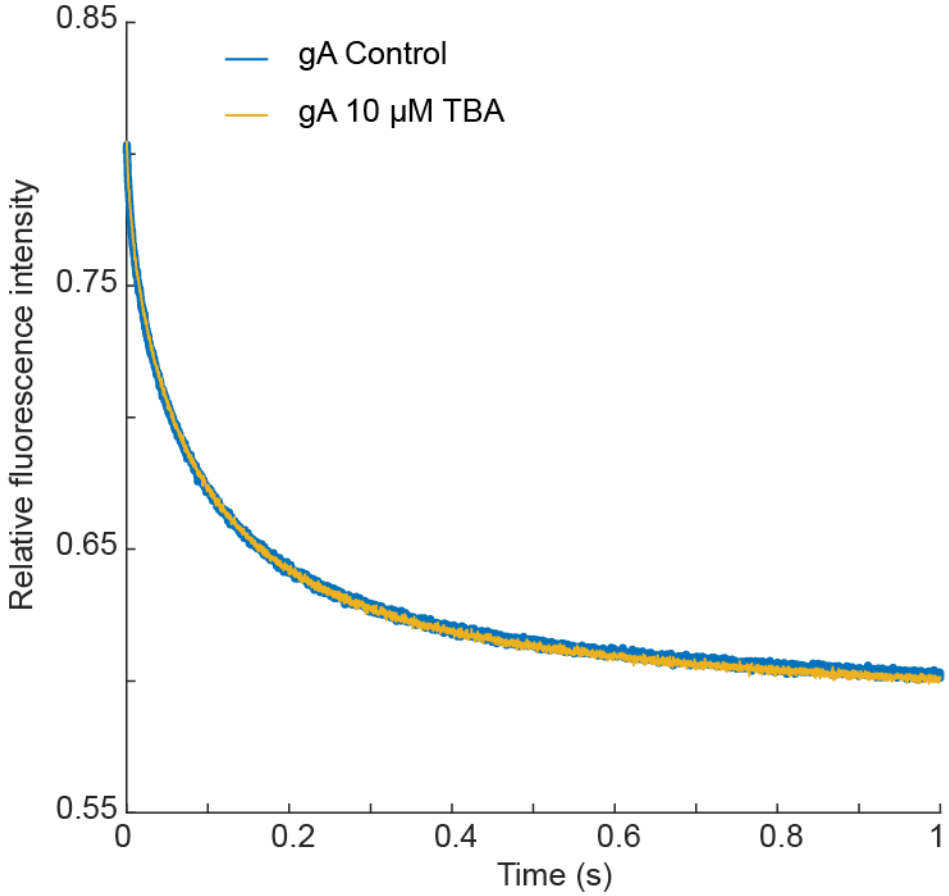

Supplemental Figure S8. TBA has no effect on gramicidin activity. Quench time-courses before (control) and after application of 10 μM TBA. Average relative change in quench rate is 1.03 ± 0.01, Mean ± SEM, $n = 4$.

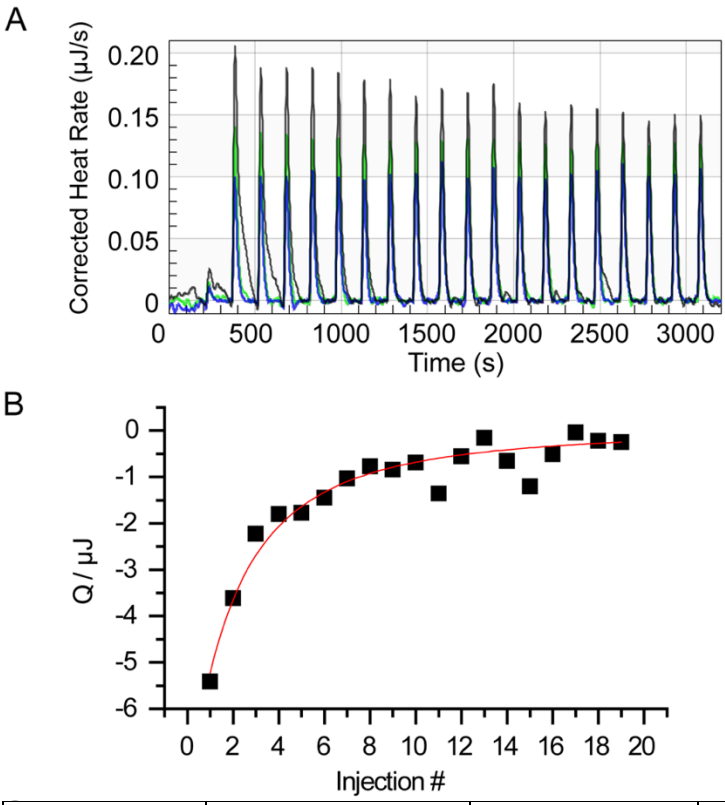

Drug	K_P	ΔH (J / mol)	ΔG	$T\Delta S$
amiodarone	23,900 ± 6,100 (9)	–5,712 ± 69	-24,310 ± 650	18,600±1,400
propranolol	576 ± 87 (4)	–7,900 ± 1,400	-15,660 ± 380	7,800 ±1,800
troglitazone	19,900 ± 2,100 (12)	–14,300 ± 3,500	-24,350 ± 290	10,000 ± 3,700

Supplemental Figure 9. Drug partitioning into lipid bilayers. (A) Black trace, heat production as function of time as 2.5 µl aliquots of a 1mM $C_{22:1}$PC LUV suspension is injected into 170 µl of a 30 µM amiodarone solution in the sample cell; green trace, heat production when the 1mM LUV suspension is injected into a drug-free buffer solution; blue trace, heat production when the buffer solution is injected into the 30 µM amiodarone solution. The area under each injection peak corresponds to the enthalpies of partitioning or dilution for that injection. (B) Injection enthalpies for 1mM LUV titration into 30 µM amiodarone, corrected for the enthalpies at saturation, as function of the injection number (black squares). The solid line denotes a fit of Eq. 1 to determine K_P. (C) Thermodynamic parameters determined from the fit for amiodarone, propranolol and troglitazone. Mean ± SEM, (*n*).

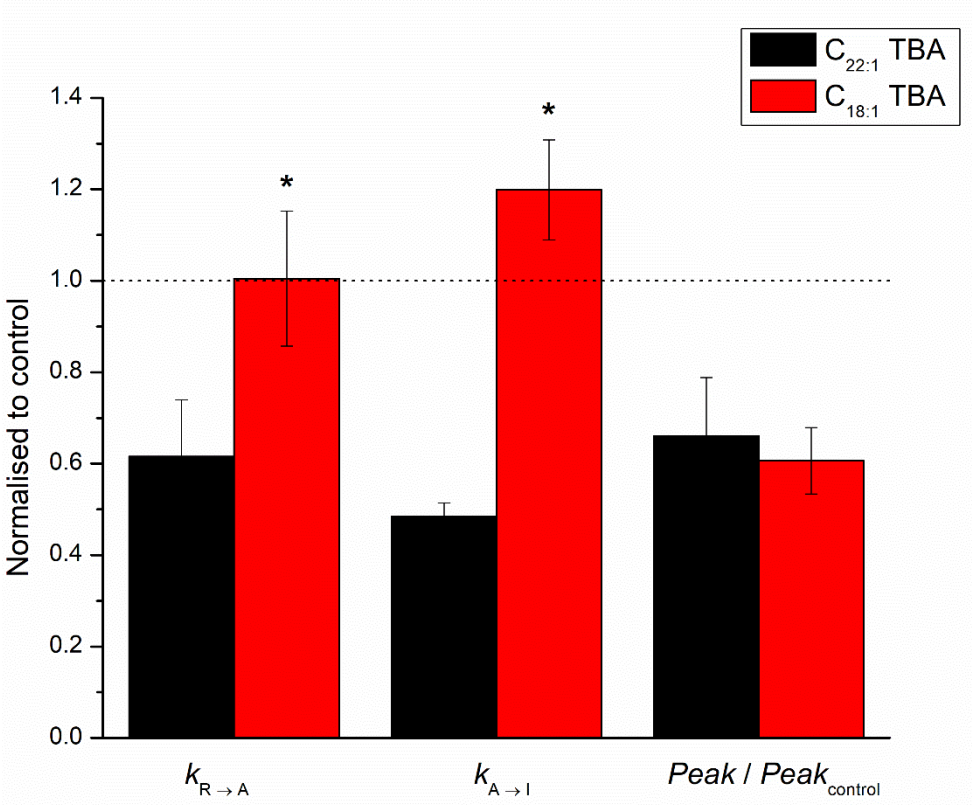

Supplemental Figure S10. Effects of TBA on KcsA function**.** KcsA reconstituted in $C_{22:1}$ (black) or $C_{18:1}$ (red) bilayers was incubated with 10 μM TBA for 10 minutes after which activation-inactivation time-course was determined (Mean ± SEM, n = 5 – 6). The difference in $k_{R\rightarrow A}$ and $k_{A\rightarrow I}$ for KcsA reconstituted in $C_{18:1}$ compared to $C_{22:1}$ is statistically significant (two-sample Student's t-test assuming equal variance P = 0.045 and 0.0003 for $k_{R\rightarrow A}$ and $k_{A\rightarrow I}$ respectively).

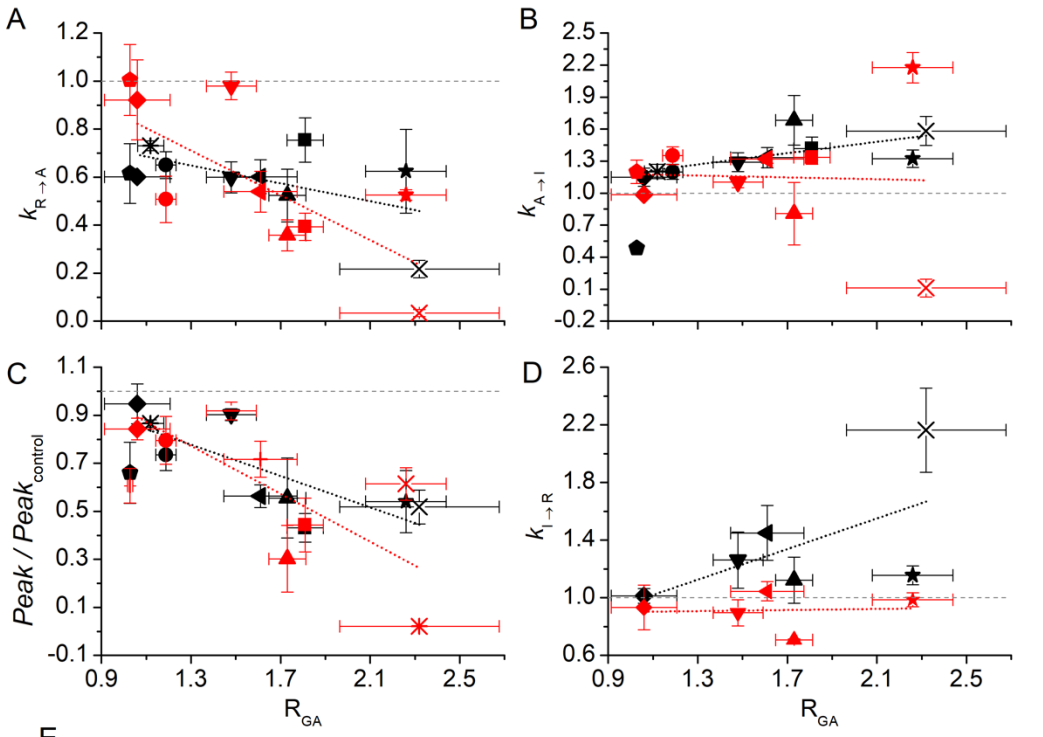

E

	Lipid	Slope	SE	Pearson's r	Adj. R^2
$k_{R\to A}$	$C_{22:1}$	-0.2	0.1	-0.6	-0.2
	$C_{18:1}$	-0.5	0.2	-0.7	0.4
$k_{A\to I}$	$C_{22:1}$	0.3	0.1	0.7	0.4
	$C_{18:1}$	-0.04	0.5	-0.03	-0.2
Peak / Peak$_{control}$	$C_{22:1}$	-0.3	0.1	-0.8	0.6
	$C_{18:1}$	-0.5	0.2	-0.7	0.5
$k_{I\to R}$	$C_{22:1}$	0.5	0.3	0.6	0.2
	$C_{18:1}$	0.02	0.2	0.1	-0.3

Supplemental Figure S11. Relations between drug-induced changes in KcsA and bilayer-modulating effect (determined using gramicidin in $C_{22:1}$ bilayers). The four panels show how (A) $k_{R\to A}$, (B) $k_{A\to I}$, (C) peak activity and (D) $k_{I\to R}$ vary as function of changes in bilayer properties produced by the same drug, quantified as R_{GA}. Gray dashed lines denote the control level. Mean ± SEM, n = 3 – 8 (Mean ± range/2 for n = 2). (E) Slopes, standard errors of fit, Pearson's ρ and Adj. R^2 for each parameter derived from the linear fits (dashed lines in panels A-D). TBA was not included in the analysis.